



Published in final edited form as:

Med Sci Sports Exerc. 2022 January 01; 54(1): 77–88. doi:10.1249/MSS.0000000000002772.

Early Onset Physical Inactivity and Metabolic Dysfunction in Tumor-bearing Mice Is Associated with Accelerated Cachexia

Brittany R. Counts, Jessica L. Halle, James A. Carson

Integrative Muscle Biology Laboratory, Division of Rehabilitation Sciences, College of Health Professions, University of Tennessee Health Science Center, Memphis TN

Abstract

Cancer-induced skeletal muscle mass loss is a critical characteristic of cachexia. While physical inactivity and systemic metabolic dysfunction can precede cachexia development, how these early-onset disruptions are related to cachexia's eventual severity is not well understood. The well-established Lewis Lung Carcinoma (LLC) pre-clinical cachexia model exhibits a varying degree of cachexia. Therefore, we examined if the early onset of physical inactivity and metabolic dysfunction were associated with accelerated cachexia development in LLC tumor-bearing mice.

METHODS: Male C57BL/6J (12 wks. age) were injected with 1×10^6 LLC cells or PBS subcutaneously in the right flank, and tissue was collected 26–28 days post cell injection. Tumor volume was measured every 5 days throughout the study to calculate the tumor growth rate. Fifteen days post tumor inoculation, a subset of PBS (n=11) and LLC (n=16) mice were individually housed in metabolic CLAMs cages for 5 days.

RESULTS: LLC mice exhibited greater body weight loss (–5.1%), decreased muscle mass (–7%), decreased fat mass (–22%), and increased plasma IL-6 (212%) compared to PBS mice. Before the onset of cachexia, total cage activity was decreased in tumor-bearing mice. Cage activity was negatively associated to tumor mass and positively associated to hindlimb muscle mass. Additionally, LLC mice had greater lipid oxidation than PBS mice.

CONCLUSION: LLC mice exhibit early-onset physical inactivity and altered systemic lipid oxidation, which are associated with the eventual development of cachexia.

Keywords

Cancer; Metabolism; Activity; Inflammation

Introduction

Lung cancer is the 2nd most common cancer type in the United States (1), with 50% of lung cancer patients developing cachexia (2). Cachexia is the unintentional loss of muscle mass with or without fat loss that is irreversible with nutritional support alone

Corresponding Author: James A. Carson, Ph.D., College of Health Professions, University of Tennessee Health Science Center, 630 Madison Avenue, Suite 633, Memphis, TN 38163, Office Phone: 901-448-5588, jcarso16@uthsc.edu.

Conflict of Interest

The authors have no conflicts of interest to report.

(3). Notably, 60% of lung cancer patients reported significant weight loss before receiving treatment, which was associated with reduced survival and increased chemotherapy toxicity (4). The high prevalence of cachexia in lung cancer patients before receiving treatment provides a solid rationale for the need to advance our understanding of the regulation of the early drivers of cachexia development occurring before treatment. Due to limitations in studying lung cancer patients, preclinical cancer models have provided valuable mechanistic insight into cachexia regulation. The Lewis Lung Carcinoma (LLC) model is a widely used syngeneic model to evaluate cachexia (5). A strength of the LLC model is its established heterogeneity in the development of cachexia (6) which has allowed for examination of early-onset events through the development of severe cachexia (7, 8). Studies using the LLC model have demonstrated the importance of several skeletal muscle signaling pathways regulating muscle mass (9–13). Impaired muscle mitochondria function precedes cachexia development (7), suggesting that understanding muscle metabolism before wasting is essential (14). Moreover, LLC mice exhibit disrupted systemic insulin and glucose signaling (15, 16) and impaired energy expenditure (17) before muscle mass changes. Disruptions to whole-body metabolic homeostasis with cachexia progression are reported in several preclinical models (18–20). These disruptions suggest early disturbances to systemic metabolism have a role in cachexia development (21) and investigation of these early metabolic changes in the LLC cachexia model is warranted.

Lung cancer patients exhibit increased energy expenditure associated with bodyweight loss (22); however, discrepancies still exist between the relationship of whole-body metabolism to disease-free survival. For example, both hypometabolic (23) and hypermetabolic (21, 24) lung cancer patients have decreased survival. Recent studies have reported increased lipid oxidation in cachectic patients (25) and pre-clinical cachexia models (26, 27). Cachectic LLC mice have increased lipolysis (28) and studies have demonstrated that lipase inhibition can preserve muscle and fat mass (15). These data and other studies report the preservation of fat mass on improved indices of cachexia (29). However, it remains unclear if altered lipid metabolism is a consequence of cachexia or precedes cachexia development, and the relationship between cachexia development and whole-body metabolism requires further investigation.

Physical activity is a daily behavior that impacts the physiological regulation of the systemic environment, individual tissues, and cells. Collectively, cachectic cancer patients and tumor-bearing mice consistently demonstrate a substantial reduction in physical activity (30–32). It is well established that activity levels can have a significant role in cancer's etiology, and recent clinical work highlighting sedentary behavior is associated with more severe cachexia (33). However, physical inactivity is often characterized as an outcome of wasting rather than a contributor to the wasting process. Decreased physical activity can precede cachexia development (18, 34, 35) and early changes in activity level are associated with the eventual severity of cachexia (36). Alternatively, several effects of increased physical activity on preventing cachexia development have been extensively examined (36–39). There is clear therapeutic potential for increased physical activity (40) or exercise to prevent or attenuate cachexia in preclinical cancer models (41, 42). While physical activity level has established effects on systemic and muscle metabolism it is currently unknown if these

early declines in physical activity are linked to cancer-induced metabolic dysfunction during cachexia initiation.

There is sufficient evidence that physical activity level has a role in cancer cachexia's progression. Since cachectic cancer patients and tumor-bearing mice demonstrate whole-body (15–17) and tissue-specific metabolic dysfunction (43), it is within reason to speculate that cancer cachexia's disruptions to physical activity are contributing to metabolic dysfunction. Furthermore, tumor development and growth in pre-clinical cancer cachexia models are related to cachexia development (18, 35, 44). Therefore, the purpose of this study was to examine if the early onset of physical inactivity and metabolic dysfunction were associated with accelerated cachexia development in LLC tumor-bearing mice. We hypothesized that the early onset of physical inactivity and metabolic dysfunction would be associated with accelerated cachexia development. To this end, we examined cachexia development in male C57Bl/6J mice inoculated with LLC cells. Fifteen days post tumor inoculation, at the onset of palpable tumors and before cachexia development, mice were housed in metabolic cages and then subsequently followed for tumor growth and cachexia development until the end of the study.

Methods

Animals

Male C57BL/6J (B6; N=62) mice were originally purchased from The Jackson Laboratory (Bar Harbor, ME, USA) and bred at the University of Tennessee Health Science Center Animal Resource Facility. Mice were kept on a 12:12h light/dark cycle beginning at 6:00AM and were given rodent chow *ad libitum* (Harlan Teklad Rodent Diet, #8604, Harlan, Indianapolis, IN, USA). All experiments were approved by the University of Tennessee Health Science Center Animal Care and Use Committee.

Lewis Lung Carcinoma Cell Inoculation

Between 11-12 weeks of age, B6 mice were injected with either phosphate buffered saline (PBS) or 1×10^6 Lewis Lung Carcinoma (LLC) cells (ATCC CRL-1642) subcutaneously in the right flank and mice were under anesthesia (isoflurane) for less than 3 minutes (10). A total of 38 mice were injected with LLC cells and 24 mice were injected with PBS.

Lewis Lung Carcinoma Animal and Tumor Monitoring

Eighty-six percent of the LLC injected mice reached the study's endpoint. Endpoint criteria were derived from previous published literature (7, 10) and veterinary guidelines for humane care of animals as follows: (1) mouse reached 30 days post tumor inoculation, (2) >20% body weight loss from day 10 after day 25 post tumor inoculation, (3) had a tumor >3cm in width or length after day 25 post tumor inoculation, or (4) the tumor was close to breaking through the skin (ulcerated) after day 25. Once an endpoint was achieved, the mouse was prepared for tissue collection and euthanized within 24 hrs. Between 10-15 days post tumor inoculation, 4 mice had tumors ulcerate and were not included in the analysis and 1 mouse died unexpectedly on day 22. To be included in the study, mice needed to achieve at least 25 days post tumor inoculation (7, 10). Therefore, a total of 33 male LLC injected mice were

used in these experiments. Tumor volume and body weight were measured every 5 days (Figure 1A). Tumor volume was calculated by the same investigator using a caliper and the following equation: $\frac{1}{2} (\text{width}^2 \times \text{length})$ (45). Additionally, we accounted for tumor growth rate throughout the study by calculating the slope of tumor volume between days 15-25.

Tissue Collection

At time of sacrifice mice were anesthetized and ~500 ul of retro-orbital blood was collected. Following eye bleeds, under anesthesia mice underwent cervical dislocation and muscles were immediately excised within 4 minutes. A second method of euthanasia was heart removal, and then organs were collected. Hindlimb muscles and organs were rapidly excised, cleared for excessive connective tissue, weighed, and snap-frozen in liquid nitrogen (46). Hindlimb muscles included were soleus, plantaris, gastrocnemius, tibialis anterior, and extensor digitorum longus.

Body Composition and Indirect Calorimetry

Fifteen days post tumor inoculation, a subset of mice (PBS n=11, LLC n=16) were individually housed and placed in the Comprehensive Laboratory Animal Monitoring System (CLAMs) cages for 5-consecutive days (47). To allow for acclimatization, the first 24hrs were removed from the analysis and the average of days 2, 3, and 4 were used for analysis. Mice were removed from the cages on day 5. Data is presented as daily average, and the average of each light and dark cycle. In mice, light cycle refers to the time when mice are resting (rest phase) and consuming little to no food. While the dark cycle, refers to the active phase when they consume most of their daily food consumption (36, 48). Prior to individual housing, mice were weighed between 7:00-9:00 AM and body composition was determined in conscious mice by magnetic resonance (EchoMRI 1100, EchoMRI, Houston, TX). Using the CLAMs system (Columbus Instruments, Columbus, OH) physical activity, oxygen consumption (VO₂), carbon dioxide production (VCO₂), and respiratory exchange ratio (RER; VCO₂/VO₂) were determined. Physical activity was quantified as the 3-day average of the hourly sum of XY beam breaks. The temperature was maintained at 22°C throughout the experiment. The Lusk equation in Oxymax software (Columbus Instruments, Columbus, OH) was used to determine energy expenditure. Carbohydrate and lipid oxidation were based on published equations that assume negligible protein oxidation (49). Before use in the equation, VO₂ and VCO₂ were converted from milliliters per kilogram lean mass per hour to milliliters per minute. Equations are as follows: carbohydrate oxidation (g/min): $(4.585 \text{ VCO}_2) - (3.226 \text{ VO}_2)$ and lipid oxidation (g/min) $(1.695 \text{ VO}_2) - (1.701 \text{ VCO}_2)$, and negative values indicate unusable time points which were removed from the analysis.

Plasma Interleukin-6 (IL-6)

Immediately prior to sacrifice, blood was collected via retro-orbital sinus with heparinized capillary tubes, placed on ice, and centrifuged (10,000g for 10 min at 4°C) (46). The supernatant was removed, and plasma IL-6 concentrations were determined using an enzyme-linked immunosorbent assay kit according to the manufacturer's instructions (Catalog #KMC0061, ThermoFisher Scientific, Waltham, MA).

Statistical Analysis

All results are reported as means \pm standard error of the mean (SEM). Students unpaired t-test were used to compare PBS and LLC mice animal characteristics and metabolic phenotyping. One-way repeated-measures ANOVA was used to examine tumor volume over time in LLC mice. Two-way repeated-measures ANOVA was used to compare tumor (PBS and LLC) to cycle (Light and Dark Cycle) for physical activity and metabolic outcomes. When necessary, Tukey's post hoc analysis was used. Pearson correlation coefficients were used to determine associations. Sample size of 6-7 per group was estimated from previous publications to ensure $p < 0.05$ at a power of 95% (17, 18). Statistical analysis was performed using GraphPad (Prism 8 for Mac OS X, La Jolla, Ca). Stepwise linear regression was used to predict metabolic parameters and indices of cachexia. Shapiro-Wilk test was used to confirm normal distribution. There was no concern regarding multi-collinearity among predictor variables in the stepwise linear regression models. Data was analyzed using SPSS statistical package (IBM SPSS Statistics 20). The level of significance for all measures was set at $p = 0.05$.

Study Approval

All experiments were approved by the University of Tennessee Health Science Center's Institutional Animal Care and Use Committee (protocol #19.001).

Results

Animal Characteristics

There were no differences in age or study duration between PBS (N=24) and LLC (N=33) mice. The study was initiated at approximately 12 weeks of age and completed at approximately 15 to 16 weeks of age. PBS and LLC mice bodyweights were not different before tumor inoculation ($p=0.848$) or 10 days post tumor inoculation ($p=0.473$). While there were no differences in absolute body weight at the end of the study ($p=0.433$), after accounting for tumor mass, LLC mice had decreased body weight compared to PBS ($p=0.004$). LLC mice had a greater body weight change from day 10 when accounting for tumor mass (-4.9%) compared to PBS (0.5%) (Figure 1B). Body weight change from day 10 was chosen because the tumor is initially palpable but before the rapid tumor growth phase (day 15-25). LLC mice had decreased gastrocnemius (Table 1; $p=0.021$) and total hindlimb muscle mass (Figure 1C; $p=0.014$) compared to PBS. LLC mice had increased spleen mass (Figure 1E) compared to PBS. Furthermore, LLC mice exhibited additional indices of cachexia when compared to PBS mice, including decreased epididymal fat mass (eWAT; Figure 1D) and decreased seminal vesicle mass (Figure 1F). The LLC mice demonstrated an early cachectic phenotype determined by mild weight loss, muscle mass and fat mass loss. However, we report a pronounced heterogeneity in the range of cachexia in this cohort of LLC mice.

LLC Tumor Mass and Growth Rate

Tumor volume was measured every 5 days throughout the study and was measurable 10 days post tumor inoculation (Figure 2A). Utilizing the LLC model's rapid tumor growth

phase, we calculated the slope of tumor growth from days 15-25. Tumor growth rate ranged from 0.036 to 0.385 cm³/5days (Figure 2B). Tumor mass ranged from 0.389 to 5.48 grams (Figure 2C). Tumor growth rate and tumor mass were correlated (Figure 2D). We compared standard indices of cachexia to each mouse's tumor mass. Tumor mass was associated with bodyweight change from day 10 (Figure 2E), hindlimb muscle mass (Figure 2G), and eWAT ($R^2=0.196$, $r=-0.442$, $p=0.010$). Interestingly, despite the range of tumor growth present, tumor growth rate was not associated to bodyweight change from day 10 (Figure 2F), hindlimb muscle mass (Figure 2H) or eWAT ($R^2=0.057$, $r=-0.238$, $p=0.182$). These data provide evidence that tumor mass at the end of the study is strongly associated with several indices of cachexia.

Relationship of Plasma IL-6 on Tumor Size and Growth and Indices of Cachexia

LLC mice had increased plasma IL-6 (212%; Figure 3A) compared to PBS mice. Plasma IL-6 was associated to tumor mass (Figure 3B), but not tumor growth rate (Figure 3C). When accounting for the 1 outlier (40pg/mL), the interpretation was unchanged by removal of the outlier (tumor mass: $R^2=0.291$, $r=0.539$, $p=0.001$ and tumor growth rate: $R^2=0.012$, $r=0.110$, $p=0.551$). Interestingly, plasma IL-6 was associated to body weight change from day 10 ($R^2=0.123$, $r=-0.350$, $p=0.046$), however this associated was due to the outlier (outlier removed: $R^2=0.019$, $r=-0.139$, $p=0.450$). Plasma IL-6 was strongly associated to hindlimb muscle mass (Figure 3D; outlier removal: $R^2=0.539$, $r=-0.734$, $p<0.001$). Furthermore, eWAT mass was associated to plasma IL-6 ($R^2=0.285$, $r=-0.534$, $p=0.001$; interpretation unchanged by outlier removal). These data provide evidence that plasma IL-6 is linked to tumor mass and some indices of cachexia.

Effect of Tumor Size and Growth on Whole Body Metabolism

In a subset of mice (PBS N=11; LLC N=16) from the large cohort, PBS and LLC mice were single housed in the CLAMs system for 5 consecutive days starting at 15 days post tumor inoculation (Figure 4A). Notably, the CLAMs mice were representative of the entire LLC cohort (see Table, Supplemental Digital Content 1, Animal Characteristics at the end of study of mice placed in the CLAMs). Metabolic parameters were similar between PBS and LLC mice 15 days post tumor inoculation (Table 2). Regarding fuel utilization, carbohydrate oxidation increased during the dark cycle in both the PBS and LLC mice compared to the light cycle, and there was no effect of LLC (Figure 4C). Lipid oxidation decreased during the dark cycle in both PBS and LLC mice compared to the light cycle (Figure 4D). Interestingly, lipid oxidation, early in tumor development, was increased in LLC mice compared to PBS mice. Lipid oxidation was not associated to tumor mass at the end of the study (Figure 4E) or tumor growth rate (Figure 4F). LLC mice metabolic parameters were compared to cachexia indices at the end of the study. Stepwise linear regression demonstrated that lipid and carbohydrate oxidation were significant predictors of plasma IL-6 (see Table, Supplemental Digital Content 2, Relationship of Metabolic Parameters and Indices of Cachexia in LLC Mice). Furthermore, lipid oxidation was negatively associated with hindlimb muscle mass (Figure 4G) and trending to be associated with plasma IL-6 (Figure 4H; outlier removal $R^2=0.204$, $r=0.451$, $p=0.105$). These data supply evidence that early metabolic disruptions related to lipid oxidation in LLC tumor-bearing are associated with more cachexia indices rather than tumor development.

Effect of Tumor Size and Growth on Physical Inactivity

We examined cage activity levels in LLC mice. Overall, LLC mice decreased cage activity by 30% compared to PBS mice (Table 2). Cage activity showed diurnal regulation (Figure 5A). Dark cycle cage activity was higher than light cycle activity for both PBS and LLC mice. However, LLC mice exhibited decreased dark cycle cage activity compared to PBS mice. LLC mice cage activity at day 15, early in tumor development, was negatively associated with tumor mass (Figure 5B) and plasma IL-6 (Figure 5E; outlier removal $R^2=0.387$, $r=-0.666$, $p=0.018$) at the end of the study. LLC mice cage activity at day 15 was not associated to tumor growth rate (Figure 5C). LLC mice cage activity at day 15 was also positively associated with hindlimb muscle (Figure 5D) and fat mass (Table 3) at the end of the study. Therefore, physical inactivity is an early manifestation of more severe cachexia indices. Stepwise linear regression demonstrated that lipid oxidation and total activity were significant predictors of hindlimb muscle mass (see Table, Supplemental Digital Content 2, Relationship of Metabolic Parameters and Indices of Cachexia in LLC Mice). There was a negative association between cage activity and lipid oxidation ($R^2=0.333$, $r=-0.576$, $p=0.019$), but not carbohydrate oxidation ($R^2=0.151$, $r=0.389$, $p=0.137$), in LLC mice early during tumor development. Taken together, these data suggest important regulation between lipid oxidation and physical inactivity during cachexia initiation. These data provide evidence that early disruptions to physical activity levels in LLC mice precede measurable differences in tumor volume and are associated with the future development of cachexia indices.

Discussion

Cancer-induced cachexia is a debilitating wasting condition (3) reported in approximately 60% of lung cancer patients. Lung cancer patients also have a high prevalence of wasting before receiving treatment (4). Studies have established that physical inactivity (30–32) and metabolic dysfunction (21, 24) are adverse consequences of cachexia. Emerging evidence suggests that these disruptions can precede cachexia development (17, 36) and may negatively impact cachexia severity. Therefore, the purpose of this study was to examine if the early onset of physical inactivity and metabolic dysfunction were associated with accelerated cachexia development in tumor-bearing mice. We report the novel finding that early-onset physical inactivity precedes cachexia development and is associated with indices of cachexia. Additionally, we report high lipid oxidation early in tumor development is associated muscle and fat mass loss. We extend previous studies by identifying that the well-established LLC preclinical cachexia model develops a wide-ranging degree of cachexia severity. We report that tumor mass, not tumor growth rate, was associated to indices of cachexia. Our findings also highlight that early-onset physical inactivity and altered systemic lipid oxidation are associated with the eventual development of cachexia, suggesting that these early disruptions might provide behavioral and pharmacological therapeutic targets for further investigation.

Cachectic cancer patients and tumor-bearing mice consistently demonstrate a reduction in physical activity (30–32). It is well established that physical activity levels can significantly impact cancer's etiology (33). While physical inactivity has been well documented with

cancer cachexia, it is often characterized as an outcome of wasting. We extend these findings by reporting that physical inactivity occurs early during tumor development and utilizing physical activity as just an outcome of cachexia is not sufficient. Furthermore, there is sufficient data to speculate that most cancer and cancer cachexia models are examining a model of physical inactivity, which should be considered. Additionally, recent findings have hypothesized physical inactivity as a contributor to the process, further supported by decrements in physical activity preceding cachexia development (18, 34, 35) and linked to cachexia's progression (36). Utilizing the ability to examine physical inactivity early during tumor development, we extend previous studies by reporting that early-onset physical inactivity is associated to indices of cachexia at the end of study. It is within reason to speculate that physical inactivity might be used as one physical function outcome to predict cachexia development. These findings have significant implications because we may intervene to offset cachexia well before measurable phenotype and tumor progression changes. However, further research is warranted. Interestingly, plasma IL-6 at the end of the study was correlated to early onset physical inactivity. Several studies have implicated a role for IL-6 in cachexia development (38, 50). While our study was conducted in male mice, given the known differential effects of sex on cachexia progression (51) it is interesting to hypothesize if IL-6's relationship is altered in the female. Future research is warranted to determine IL-6's relationship to early onset physical inactivity. Alternatively, physical inactivity and sedentary behaviors are known to increase chronic inflammation (52). It is interesting to speculate that early physical activity decrements contribute to the wasting process by increasing inflammation. However, future studies should investigate if this is true. Several studies have examined the effect of increased physical activity on preventing cachexia progression (36–39), supporting increased activity's therapeutic potential on preventing or delaying disease onset. There is currently ample evidence that identifies physical activity level as a critical modulator of cancer cachexia's progression. It is well established that physical activity has pronounced effects on systemic metabolism and improves patients' health outcomes with chronic disease. Since cachectic cancer patients and tumor-bearing mice demonstrate whole-body (15–17) and tissue-specific metabolic dysfunction (43), it is within reason to theorize that cancer cachexia's disruptions to physical activity can directly or indirectly contribute to systemic metabolic dysfunction. We report decrements in physical activity and impaired lipid oxidation early before weight loss. During the initial phases of tumor development, the mechanistic linkage between these events remains to be established. However, early-onset physical inactivity was associated to impaired lipid oxidation and several indices of cachexia. Future studies should examine if increased physical activity once inactivity has been identified is sufficient to prevent cachexia development.

Energy expenditure is an indirect method to determine whole-body metabolism. Lung cancer patients exhibit increased energy expenditure and have been linked to greater bodyweight loss (22). Therefore, understanding the effect of whole-body metabolism and its relationship to cachexia development is needed to provide targeted therapeutics to improve patient life quality and survival. A role for hypermetabolism in cachexia development has been examined (21) and has potential as an independent prognostic risk factor for lung cancer patients (24). Results examining energy expenditure and cachexia development in

preclinical models are currently equivocal, and divergent findings may be attributed to the characteristics of the tumor and stage of cachexia examined, nutritional status, and whether the fed and fasted condition were accounted for in the study. Several preclinical cancer cachexia models have reported increased energy expenditure (17, 20, 28); however, other studies report reduced energy expenditure (18, 19). Our study provides novel insight into LLC mice metabolism before weight loss and during the initiation of rapid tumor growth. We initiated the examination of the whole-body metabolism when the LLC tumor was just beginning to be palpable. Overall, we report that LLC tumor-bearing mice at this early stage did not have altered energy expenditure or food consumption. Early measurements of energy expenditure were also not associated with cachexia indices later in the study. While this was unexpected, most preclinical studies report energy expenditure after the initiation of cachexia. Given the lack of association to cachexia development and energy expenditure, we examined if there were disruptions to diurnal fuel utilization. We extend previous studies by reporting increased lipid oxidation early in LLC tumor bearing mice. These metabolic changes have significant implications because they occurred early in tumor development, before weight loss, and were associated to hindlimb and fat mass cachexia at the end of the study. Several studies have speculated that fat loss occurs before muscle wasting and may have a role in driving initial muscle mass loss (15). The relationship between IL-6 and lipid oxidation is commonly discussed and has substantial ramifications on several diseases. We report the early increase in lipid oxidation was a predictor of plasma IL-6 at the end study, further supporting the potential relationship between lipid metabolism and IL-6. While chronically elevated IL-6 has established direct effects on muscle catabolism and anabolic suppression (53, 54), it would be within reason to speculate that IL-6 is also indirectly regulating muscle wasting through actions in adipose tissue. Additionally, it would be interesting to hypothesize the interaction between lipid oxidation and chronic systemic inflammation, which progresses during the tumor's rapid growth. These results suggest that further investigation is needed to determine if disrupted lipid metabolism is linked to cachexia initiation and progression.

Understanding cancer cachexia regulation in humans is complex due to the multifactorial regulation of wasting syndromes and the heterogeneity of the cancer type, stage, treatment, and patient characteristics. Therefore, preclinical cancer cachexia models have provided essential foundational knowledge on understanding cancer-induced wasting. Furthermore, the need to develop a multimodal approach to treating cachexia due to this complexity has been widely theorized; preclinical modeling can provide the mechanistic underpinnings for developing these approaches. The LLC tumor-bearing mouse is a widely used pre-clinical model to study cancer-induced cachexia (9–13). Published works using the LLC model to study cachexia report a significant heterogeneity in the cachexia severity developed (6). Bodyweight loss reported in published studies ranges from –20 to 3%, with many studies not reporting the variable. Studies have also used the time course of tumor development to examine cachexia stages ranging from a categorization of initiation to refractory cachexia (7, 8). The majority of studies using the LLC model have reported events late in cachexia development and coincides with mice ranging from 21-35 days post LLC tumor inoculation. It is crucial to note the evident inconsistencies in the literature on reporting body weight change and cachexia indices in implantable tumor models. Our current study provides

further evidence for the importance of accounting for LLC-induced cachexia's heterogeneity and complexity when interpreting findings.

The LLC model's heterogeneity can be viewed as advantageous in studying cachexia development when studies are powered so that they can examine different severities of cachexia induced by the same tumor type. LLC-induced cachexia in mice involves skeletal muscle mass loss ranging from -10 to -35% and fat mass loss ranging from -15 to -94% that coincides with a range of tumor mass from 1.3-5.0 grams (7-10, 12, 15, 28). We report a wide range in tumor mass, body weight change, muscle, and fat mass loss, which agrees with previously published findings. However, we have extended this understanding by reporting a significant association between higher tumor mass at the end of the study and more severe cachexia indices. Beyond tumor mass at the end of the study, we also quantified tumor growth rate during the study, which we theorized could impact cachexia initiation and progression. While tumor growth rate was associated with a tumor mass at the end of the study, tumor growth rate was not associated to indices of cachexia. It is interestingly to speculate that tumor mass is more associated to cachexia indices than tumor growth rate simply due to a greater tumor burden. While it's outside the scope of this manuscript, it's possible that tumor growth rate, while not associated to indices of cachexia, could be associated to several adverse effects of the tumor: insulin resistance, drug intolerance, metastasis, etc. However, further research is warranted to understand the implications of tumor growth rate on cachexia progression and disease-free survival. Furthermore, despite similarities in the initial LLC cells, inoculation, sex and genetic background of mice, and similar housing conditions, we report significant heterogeneity in tumor growth after day 15 of inoculation. Several studies have explored the early and late LLC cachexia events (7, 12, 15) and reported fat loss early in cachexia progression, whereas muscle wasting occurred later (12, 15). Furthermore, several studies have speculated dysfunctional muscle signaling occurs before measurable differences in muscle mass (7). Unfortunately, in preclinical studies, some critical cachexia indices can only be quantified at the study's endpoint, making it challenging to determine if early disruptions in muscle or fat regulation contribute to the eventual development of refractory cachexia (6). To this end, we report changes to systemic measurements of lipid metabolism, cage activity, and tumor mass before the development of cachexia that were associated with eventual endpoint cachexia parameters.

There is mounting evidence that physical inactivity has a role in the progression of cancer cachexia. Systemic and tissue-specific metabolic dysfunction is widely examined for regulating cancer cachexia initiation. We sought to investigate if early physical activity changes in LLC tumor-bearing mice were associated with systemic metabolic dysfunction and the eventual severity of cachexia. Therefore, we provide novel insight into the implications of early onset physical inactivity's association to cachexia indices in LLC tumor-bearing mice. We report that before the onset of cachexia, tumor bearing mice exhibited decreased cage activity and increased lipid oxidation which were associated to greater muscle mass loss at the end of the study. We also report that tumor mass at the end of study, not tumor growth rate, is strongly associated with several indices of cachexia. Taken together, our findings provide evidence that early-onset altered systemic lipid oxidation and physical inactivity are associated with the eventual development of cachexia in male mice.

Further research is warranted to determine if these early disruptions provide behavioral and pharmacological therapeutic targets to prevent or attenuate cachexia progression.

Supplementary Material

Refer to Web version on PubMed Central for supplementary material.

Acknowledgments

This work was supported by the National Institute of Health Grants RO1 CA-121249 (NCI) to J.A. Carson and American College of Sports Medicine #19-00890 to B.R. Counts. The study results are presented clearly, honestly, and without fabrication, falsification, or inappropriate data manipulation. The results of the present study do not constitute an endorsement by ACSM.

References

1. Siegel RL, Miller KD, Fuchs HE, Jemal A. Cancer Statistics, 2021. *CA Cancer J Clin*. 2021;71(1):7–33. [PubMed: 33433946]
2. Jafri SH, Prevgigliano C, Khandelwal K, Shi R. Cachexia Index in Advanced Non-Small-Cell Lung Cancer Patients. *Clin Med Insights Oncol*. 2015;9:87–93. [PubMed: 26604850]
3. Evans WJ, Morley JE, Argiles J et al. Cachexia: a new definition. *Clin Nutr*. 2008;27(6):793–9. [PubMed: 18718696]
4. Ross PJ, Ashley S, Norton A et al. Do patients with weight loss have a worse outcome when undergoing chemotherapy for lung cancers? *Br J Cancer*. 2004;90(10):1905–11. [PubMed: 15138470]
5. Kellar A, Egan C, Morris D. Preclinical Murine Models for Lung Cancer: Clinical Trial Applications. *Biomed Res Int*. 2015;2015:621324. [PubMed: 26064932]
6. Fernandez GJ, Ferreira JH, Vechetti IJ Jr. et al. MicroRNA-mRNA Co-sequencing Identifies Transcriptional and Post-transcriptional Regulatory Networks Underlying Muscle Wasting in Cancer Cachexia. *Front Genet*. 2020;11:541. [PubMed: 32547603]
7. Brown JL, Rosa-Caldwell ME, Lee DE et al. Mitochondrial degeneration precedes the development of muscle atrophy in progression of cancer cachexia in tumour-bearing mice. *J Cachexia Sarcopenia Muscle*. 2017;8(6):926–38. [PubMed: 28845591]
8. Sun R, Zhang S, Lu X et al. Comparative molecular analysis of early and late cancer cachexia-induced muscle wasting in mouse models. *Oncol Rep*. 2016;36(6):3291–302. [PubMed: 27748895]
9. Murphy KT, Chee A, Gleeson BG et al. Antibody-directed myostatin inhibition enhances muscle mass and function in tumor-bearing mice. *Am J Physiol Regul Integr Comp Physiol*. 2011;301(3):R716–26. [PubMed: 21677277]
10. Puppa MJ, Gao S, Narsale AA, Carson JA. Skeletal muscle glycoprotein 130's role in Lewis lung carcinoma-induced cachexia. *FASEB J*. 2014;28(2):998–1009. [PubMed: 24145720]
11. Bohnert KR, Goli P, Roy A et al. The Toll-Like Receptor/MyD88/XBP1 Signaling Axis Mediates Skeletal Muscle Wasting during Cancer Cachexia. *Mol Cell Biol*. 2019;39(15).
12. Chiappalupi S, Sorci G, Vukasinovic A et al. Targeting RAGE prevents muscle wasting and prolongs survival in cancer cachexia. *J Cachexia Sarcopenia Muscle*. 2020;11(4):929–46. [PubMed: 32159297]
13. Zhang G, Jin B, Li YP. C/EBPbeta mediates tumour-induced ubiquitin ligase atrogin1/MAFbx upregulation and muscle wasting. *EMBO J*. 2011;30(20):4323–35. [PubMed: 21847090]
14. Penna F, Ballaro R, Beltra M, De Lucia S, Costelli P. Modulating Metabolism to Improve Cancer-Induced Muscle Wasting. *Oxid Med Cell Longev*. 2018;2018:7153610. [PubMed: 29785246]
15. Das SK, Eder S, Schauer S et al. Adipose triglyceride lipase contributes to cancer-associated cachexia. *Science*. 2011;333(6039):233–8. [PubMed: 21680814]

16. Han X, Raun SH, Carlsson M et al. Cancer causes metabolic perturbations associated with reduced insulin-stimulated glucose uptake in peripheral tissues and impaired muscle microvascular perfusion. *Metabolism*. 2020;105:154169. [PubMed: 31987858]
17. Kir S, White JP, Kleiner S et al. Tumour-derived PTH-related protein triggers adipose tissue browning and cancer cachexia. *Nature*. 2014;513(7516):100–4. [PubMed: 25043053]
18. Murphy KT, Chee A, Trieu J, Naim T, Lynch GS. Importance of functional and metabolic impairments in the characterization of the C-26 murine model of cancer cachexia. *Dis Model Mech*. 2012;5(4):533–45. [PubMed: 22563056]
19. Tsoli M, Moore M, Burg D et al. Activation of thermogenesis in brown adipose tissue and dysregulated lipid metabolism associated with cancer cachexia in mice. *Cancer Res*. 2012;72(17):4372–82. [PubMed: 22719069]
20. Petruzzelli M, Schweiger M, Schreiber R et al. A switch from white to brown fat increases energy expenditure in cancer-associated cachexia. *Cell Metab*. 2014;20(3):433–47. [PubMed: 25043816]
21. Vazelle C, Jouinot A, Durand JP et al. Relation between hypermetabolism, cachexia, and survival in cancer patients: a prospective study in 390 cancer patients before initiation of anticancer therapy. *Am J Clin Nutr*. 2017;105(5):1139–47. [PubMed: 28356274]
22. Eden E, Ekman L, Bennegard K, Lindmark L, Lundholm K. Whole-body tyrosine flux in relation to energy expenditure in weight-losing cancer patients. *Metabolism*. 1984;33(11):1020–7. [PubMed: 6493045]
23. Jatoti A, Daly BD, Hughes V, Dallal GE, Roubenoff R. The prognostic effect of increased resting energy expenditure prior to treatment for lung cancer. *Lung Cancer*. 1999;23(2):153–8. [PubMed: 10217619]
24. Jouinot A, Ulmann G, Vazelle C et al. Hypermetabolism is an independent prognostic factor of survival in metastatic non-small cell lung cancer patients. *Clin Nutr*. 2020;39(6):1893–9. [PubMed: 31443979]
25. Zuidgeest-van Leeuwen SD, van den Berg JW, Wattimena JL et al. Lipolysis and lipid oxidation in weight-losing cancer patients and healthy subjects. *Metabolism*. 2000;49(7):931–6. [PubMed: 10910006]
26. Kliewer KL, Ke JY, Tian M, Cole RM, Andridge RR, Belury MA. Adipose tissue lipolysis and energy metabolism in early cancer cachexia in mice. *Cancer Biol Ther*. 2015;16(6):886–97. [PubMed: 25457061]
27. Hu W, Xiong H, Ru Z et al. Extracellular vesicles-released parathyroid hormone-related protein from Lewis lung carcinoma induces lipolysis and adipose tissue browning in cancer cachexia. *Cell Death Dis*. 2021;12(1):134. [PubMed: 33510128]
28. Liu H, Luo J, Guillory B et al. Ghrelin ameliorates tumor-induced adipose tissue atrophy and inflammation via Ghrelin receptor-dependent and -independent pathways. *Oncotarget*. 2020;11(35):3286–302. [PubMed: 32934774]
29. Henriques F, Lopes MA, Franco FO et al. Toll-Like Receptor-4 Disruption Suppresses Adipose Tissue Remodeling and Increases Survival in Cancer Cachexia Syndrome. *Sci Rep*. 2018;8(1):18024. [PubMed: 30575787]
30. Nissinen TA, Hentila J, Penna F et al. Treating cachexia using soluble ACVR2B improves survival, alters mTOR localization, and attenuates liver and spleen responses. *J Cachexia Sarcopenia Muscle*. 2018;9(3):514–29. [PubMed: 29722201]
31. Moses AW, Slater C, Preston T, Barber MD, Fearon KC. Reduced total energy expenditure and physical activity in cachectic patients with pancreatic cancer can be modulated by an energy and protein dense oral supplement enriched with n-3 fatty acids. *Br J Cancer*. 2004;90(5):996–1002. [PubMed: 14997196]
32. Puppa MJ, Murphy EA, Fayad R, Hand GA, Carson JA. Cachectic skeletal muscle response to a novel bout of low-frequency stimulation. *J Appl Physiol* (1985). 2014;116(8):1078–87. [PubMed: 24610533]
33. Gresham G, Hendifar AE, Spiegel B et al. Wearable activity monitors to assess performance status and predict clinical outcomes in advanced cancer patients. *NPJ Digit Med*. 2018;1:27. [PubMed: 31304309]

34. VanderVeen BN, Hardee JP, Fix DK, Carson JA. Skeletal muscle function during the progression of cancer cachexia in the male Apc(Min/+) mouse. *J Appl Physiol* (1985). 2018;124(3):684–95. [PubMed: 29122966]
35. Baltgalvis KA, Berger FG, Pena MM, Mark Davis J, White JP, Carson JA. Activity level, apoptosis, and development of cachexia in Apc(Min/+) mice. *J Appl Physiol* (1985). 2010;109(4):1155–61. [PubMed: 20651218]
36. Counts BR, Hardee JP, Fix DK, Vanderveen BN, Montalvo RN, Carson JA. Cachexia Disrupts Diurnal Regulation of Activity, Feeding, and Muscle Mechanistic Target of Rapamycin Complex 1 in Mice. *Med Sci Sports Exerc*. 2020;52(3):577–87. [PubMed: 32058469]
37. Vanderveen BN, Fix DK, Counts BR, Carson JA. The Effect of Wheel Exercise on Functional Indices of Cachexia in Tumor-bearing Mice. *Med Sci Sports Exerc*. 2020;52(11):2320–30. [PubMed: 33064407]
38. Puppa MJ, White JP, Velazquez KT et al. The effect of exercise on IL-6-induced cachexia in the Apc (Min/+) mouse. *J Cachexia Sarcopenia Muscle*. 2012;3(2):117–37. [PubMed: 22476915]
39. Pigna E, Berardi E, Aulino P et al. Aerobic Exercise and Pharmacological Treatments Counteract Cachexia by Modulating Autophagy in Colon Cancer. *Sci Rep*. 2016;6:26991. [PubMed: 27244599]
40. Fix DK, Counts BR, Smuder AJ, Sarzynski MA, Koh HJ, Carson JA. Wheel running improves fasting-induced AMPK signaling in skeletal muscle from tumor-bearing mice. *Physiol Rep*. 2021;9(14):e14924. [PubMed: 34270178]
41. Hardee JP, Counts BR, Carson JA. Understanding the Role of Exercise in Cancer Cachexia Therapy. *Am J Lifestyle Med*. 2019;13(1):46–60. [PubMed: 30627079]
42. Halle JLCB, Carson JA. Exercise as a Therapy for Cancer-Induced Muscle Wasting. *Sports Medicine and Health Science*. 2020;2(4):186–94.
43. Fonseca G, Farkas J, Dora E, von Haehling S, Lainscak M. Cancer Cachexia and Related Metabolic Dysfunction. *Int J Mol Sci*. 2020;21(7).
44. Banh T, Snoke D, Cole RM, Angelotti A, Schnell PM, Belury MA. Higher tumor mass and lower adipose mass are associated with colon26 adenocarcinoma-induced cachexia in male, female and ovariectomized mice. *Oncol Rep*. 2019;41(5):2909–18. [PubMed: 30896836]
45. Jensen MM, Jorgensen JT, Binderup T, Kjaer A. Tumor volume in subcutaneous mouse xenografts measured by microCT is more accurate and reproducible than determined by 18F-FDG-microPET or external caliper. *BMC Med Imaging*. 2008;8:16. [PubMed: 18925932]
46. Hardee JP, Counts BR, Gao S et al. Inflammatory signalling regulates eccentric contraction-induced protein synthesis in cachectic skeletal muscle. *J Cachexia Sarcopenia Muscle*. 2018;9(2):369–83. [PubMed: 29215198]
47. Stephenson EJ, Ragauskas A, Jaligama S et al. Exposure to environmentally persistent free radicals during gestation lowers energy expenditure and impairs skeletal muscle mitochondrial function in adult mice. *Am J Physiol Endocrinol Metab*. 2016;310(11):E1003–15. [PubMed: 27117006]
48. Jensen TL, Kiersgaard MK, Sorensen DB, Mikkelsen LF. Fasting of mice: a review. *Lab Anim*. 2013;47(4):225–40. [PubMed: 24025567]
49. Peronnet F, Massicotte D. Table of nonprotein respiratory quotient: an update. *Can J Sport Sci*. 1991;16(1):23–9. [PubMed: 1645211]
50. Narsale AA, Carson JA. Role of interleukin-6 in cachexia: therapeutic implications. *Curr Opin Support Palliat Care*. 2014;8(4):321–7. [PubMed: 25319274]
51. Hetzler KL, Hardee JP, Puppa MJ et al. Sex differences in the relationship of IL-6 signaling to cancer cachexia progression. *Biochim Biophys Acta*. 2015;1852(5):816–25. [PubMed: 25555992]
52. Booth FW, Roberts CK, Laye MJ. Lack of exercise is a major cause of chronic diseases. *Compr Physiol*. 2012;2(2):1143–211. [PubMed: 23798298]
53. Bonetto A, Aydogdu T, Jin X et al. JAK/STAT3 pathway inhibition blocks skeletal muscle wasting downstream of IL-6 and in experimental cancer cachexia. *Am J Physiol Endocrinol Metab*. 2012;303(3):E410–21. [PubMed: 22669242]
54. Carson JA, Baltgalvis KA. Interleukin 6 as a key regulator of muscle mass during cachexia. *Exerc Sport Sci Rev*. 2010;38(4):168–76. [PubMed: 20871233]

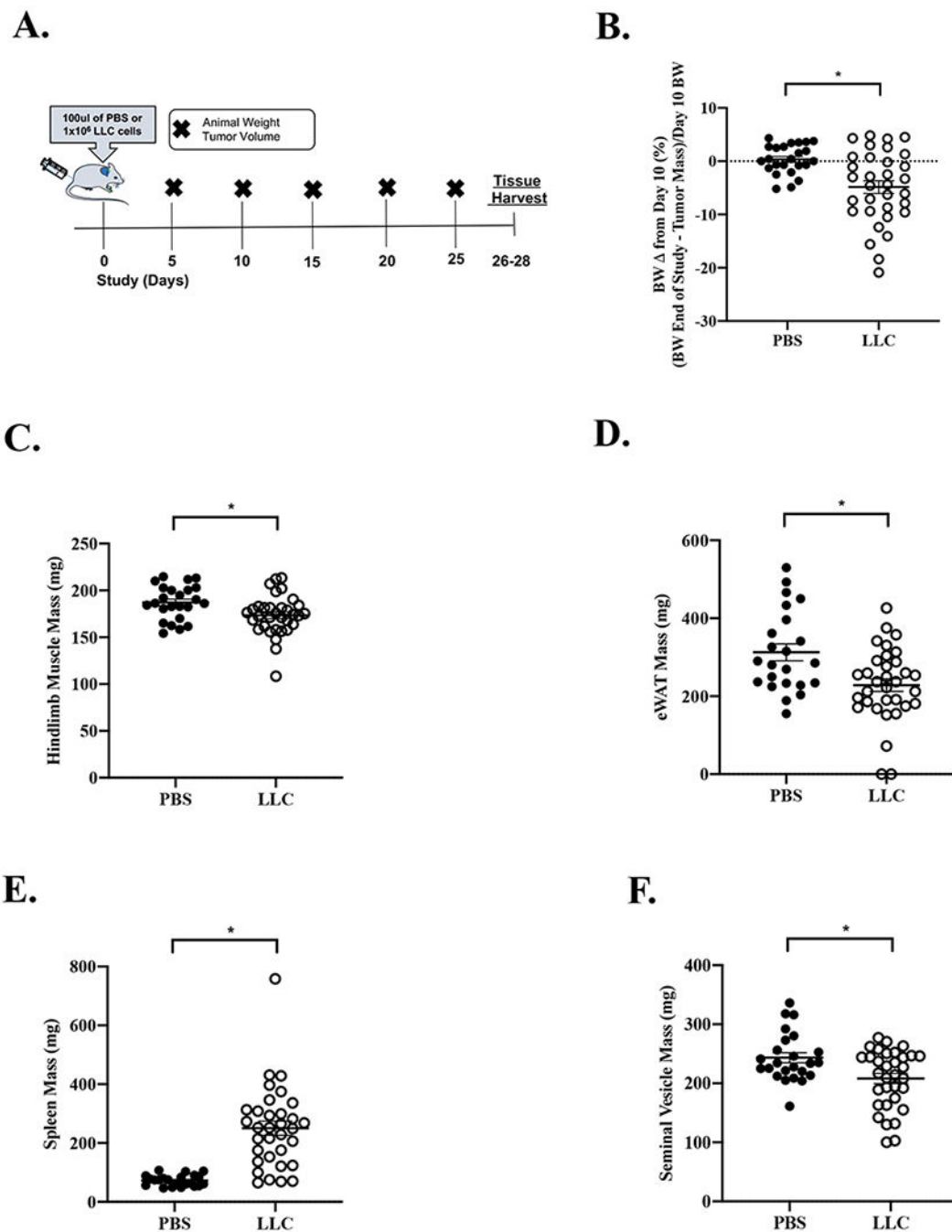


Figure 1: Effect of Lewis Lung Carcinoma (LLC) Tumor on Indices of Cachexia.

Data is expressed as mean (SEM). A. Study Design. B. Body weight change from Day 10 post tumor inoculation. Body weight is calculated as the sacrifice body weight minus the tumor mass divided by day 10 body weight. C. Total hindlimb muscle mass. D. eWAT mass. E. Spleen mass. F. Seminal Vesicle mass. Abbreviations: BW: body weight, mg: milligrams, eWAT: epididymal white adipose tissue, PBS: phosphate buffered saline, LLC: Lewis Lung Carcinoma. Unpaired t-test was used to compare PBS to LLC. * Different than PBS. Statistical significance was set a $p < 0.05$. $N = 24-33$ per group.

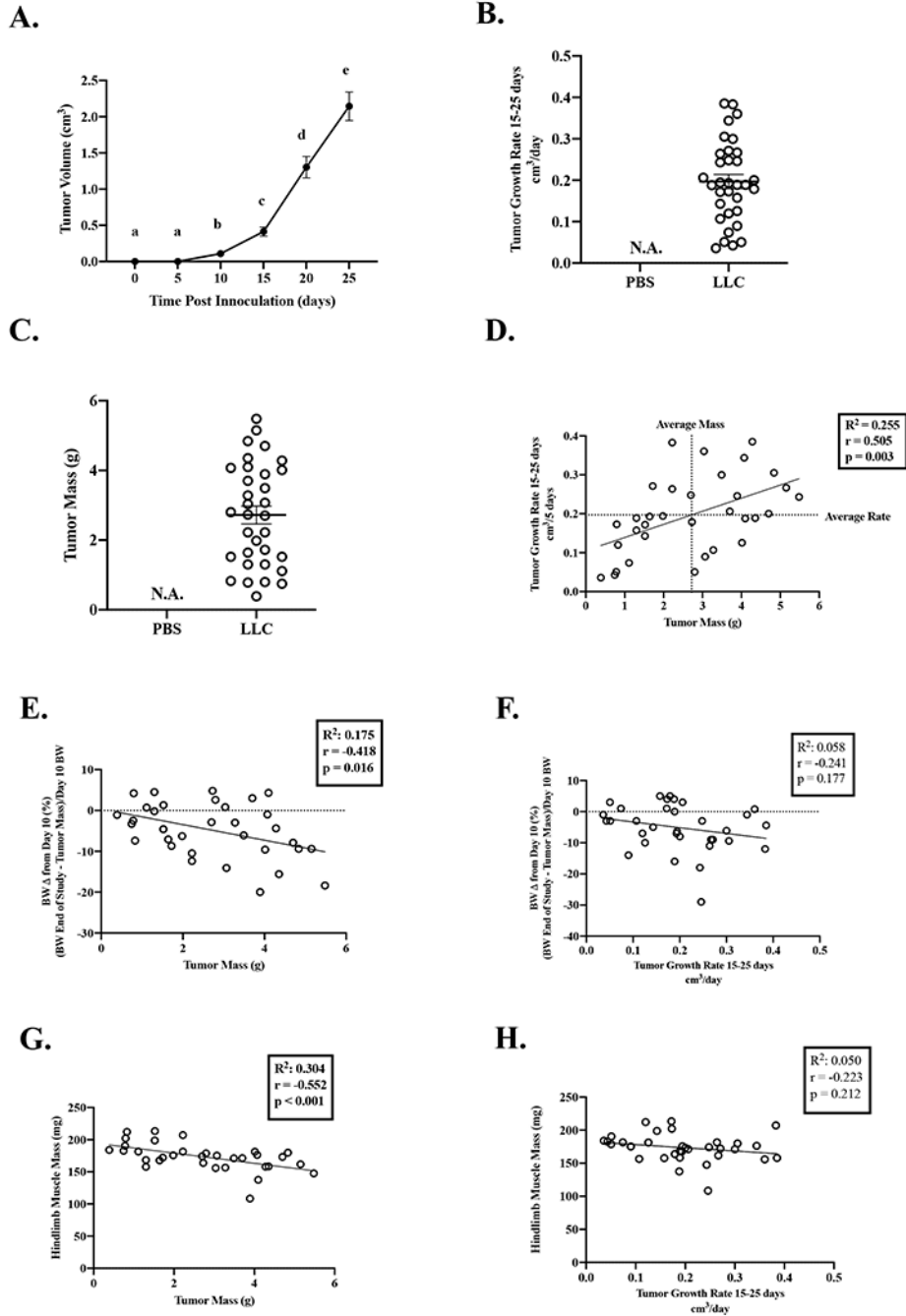


Figure 2: Effect of Tumor Size and Growth Rate on Indices of Cachexia

Data is expressed as mean (SEM). A. Tumor Volume over the course of the study. N=33. B. Tumor Growth Rate. C. Tumor Mass. D. Tumor growth rate correlated to tumor mass. E. Body weight change from day 10 correlated to tumor mass. F. Body weight change from day 10 correlated to tumor growth rate. G. Hindlimb muscle mass correlated to tumor mass. H. Hindlimb muscle mass correlated to tumor growth rate. Abbreviations: BW: body weight, mg: milligrams, cm³: centimeters cubed, g: grams: PBS: phosphate buffered saline, LLC: Lewis Lung Carcinoma. One-way repeated measures ANOVA was used to compare tumor

volume over time (Figure A). Different letters mean different between groups. Pearson Correlation Coefficient was used for correlations (Figures D-H). Statistical significance was set a $p < 0.05$. $N = 33$.

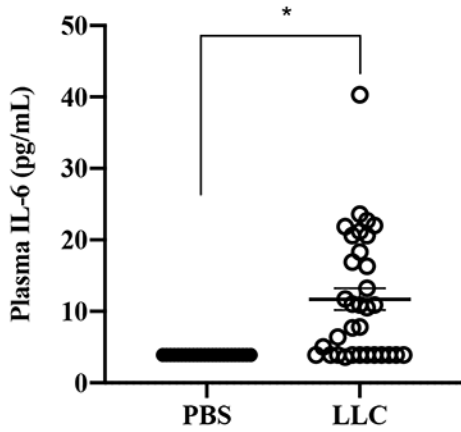
Author Manuscript

Author Manuscript

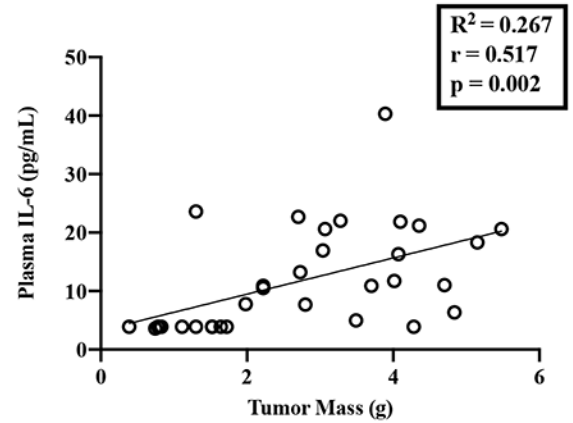
Author Manuscript

Author Manuscript

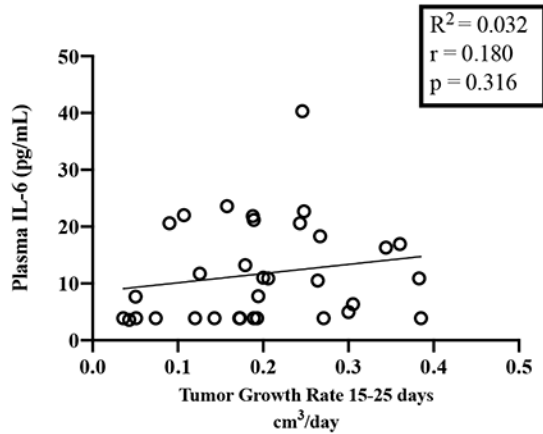
A.



B.



C.



D.

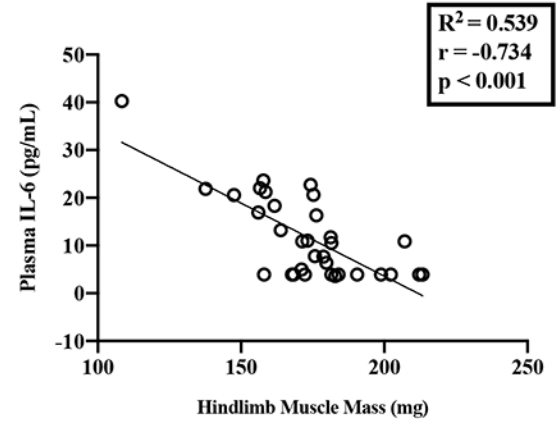


Figure 3:
 Relationship of Plasma IL-6 on Tumor Size and Growth and Indices of Cachexia
 Data is expressed as mean (SEM). A. Plasma IL-6. B. Plasma IL-6 correlated to tumor mass. C. Plasma IL-6 correlated to tumor growth rate. D. Plasma IL-6 correlated to hindlimb muscle mass. Abbreviations: BW: body weight, pg/mL: picograms per milliliter, mg: milligrams, g: grams, PBS: phosphate buffered saline, LLC: Lewis Lung Carcinoma, cm³: centimeters cubed. Plasma IL-6 of 3.9pg/mL is used for undetected values per manufacturer’s instructions. Unpaired t-test was used to compare PBS to LLC (Figures A). * Different than PBS. Pearson Correlation Coefficient was used for correlations (Figure B-D). Statistical significance was set a p<0.05.

Author Manuscript

Author Manuscript

Author Manuscript

Author Manuscript

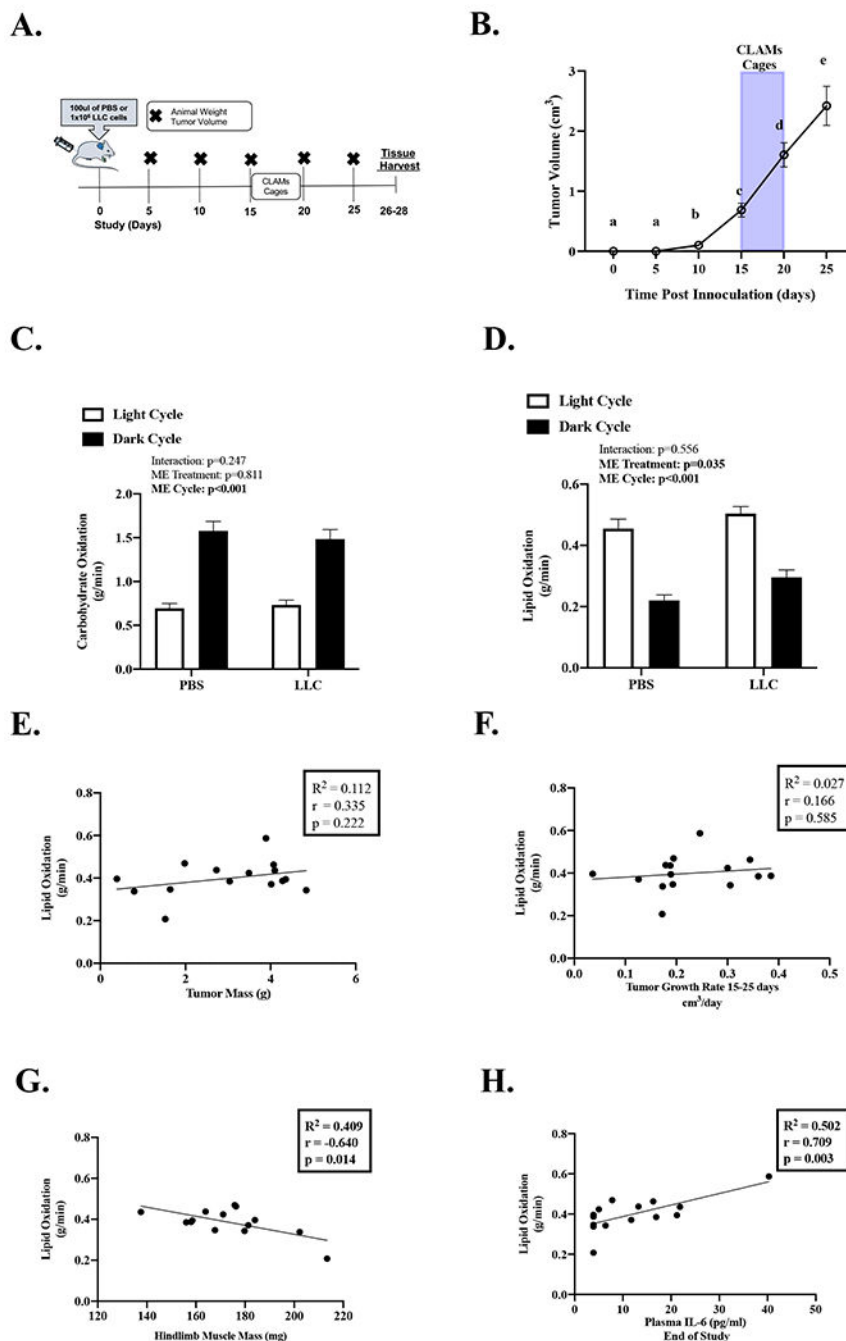


Figure 4: Effect of Tumor Size and Growth on Whole Body Metabolism

Data is expressed as mean (SEM). A. Study Design. B. Tumor Volume over the course of the study in mice placed in the CLAMs Unit. Grey bar indicates when mice were placed in the CLAMs Unit. N=16. C. Average carbohydrate oxidation in grams per minute per light and dark cycle. N:11-16 per group. D. Average lipid oxidation in grams per minute per light and dark cycle. N:11-16 per group. E. Average daily lipid oxidation correlated to tumor mass. F. Average daily lipid oxidation correlated to tumor growth rate. G. Average daily lipid oxidation correlated to hindlimb muscle mass. H. Average daily lipid oxidation

correlated to plasma IL-6. Abbreviations: ME: Main effect, pg/mL: picograms per milliliter, mg: milligrams, g: grams, PBS: phosphate buffered saline, LLC: Lewis Lung Carcinoma, cm³: centimeters cubed, g/min: grams per minute. One-way repeated measures ANOVA was used to compare tumor volume over time (Figure B). Different letters mean different between groups. Two-way repeated measures ANOVA (2-time points x 2 treatments) was used to compare fuel oxidation during the light and dark cycle. (Figures C, D). Pearson Correlation Coefficient was used for correlations (Figure E-H). Statistical significance was set a $p < 0.05$.

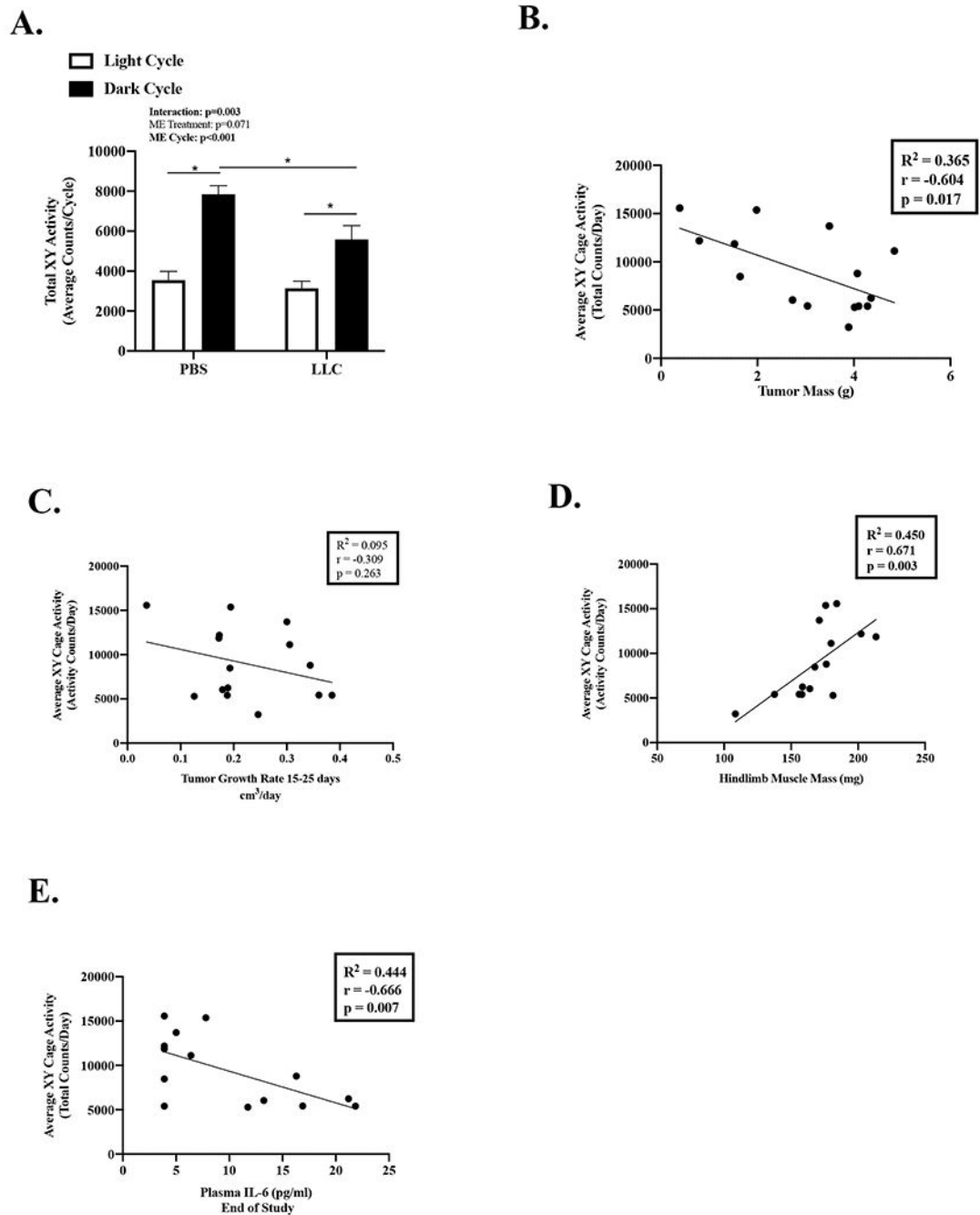


Figure 5: Effect of Tumor Size and Rate on Physical Activity

Data is expressed as mean (SEM). A. Total Cage XY Activity Counts expressed as 3-day average of the total activity counts per cycle. N=11-16 per group. B. Average XY Cage Activity correlated to tumor mass. C. Average XY Cage Activity correlated to tumor growth rate. D. Average XY Cage Activity correlated to hindlimb muscle mass. E. Average XY Cage Activity correlated to plasma IL-6. Abbreviations: ME: main effect, PBS: phosphate buffered saline, LLC: Lewis Lung Carcinoma, pg/mL: picograms per milliliter, g/min: grams per minute. Two-way repeated measures ANOVA (2-time points x 2 treatments) was used

to compare cage activity during the light and dark cycle. (Figure A). Pearson Correlation Coefficient was used for correlations (Figures B-E). Statistical significance was set a $p < 0.05$.

Author Manuscript

Author Manuscript

Author Manuscript

Author Manuscript

Table 1:

Effect of LLC on Animal Characteristics

Treatment	PBS	LLC
N	24	33
Tumor Inoculation Age (wks.)	11.8 (0.1)	11.5 (0.1)
Study Duration (days)	26.4 (0.3)	26.1 (0.3)
End of Study Age (wks.)	15.6 (0.1)	15.2 (0.1)
BW Pre Tumor Inoculation (g)	24.9 (0.5)	24.8 (0.4)
BW Day 10 of Study (g)	26.2 (0.4)	25.8 (0.4)
BW End of Study (g)	26.7 (0.4)	27.1 (0.3)
Tumor Mass (g)	-	2.7 (0.5)
BW End of Study – Tumor Mass (g)	26.7 (0.4) [^]	24.4 (0.5) *
Tumor Growth Rate 15-25days (cm³/5 days)	-	0.197 (0.017)
Gastrocnemius Mass (mg)	115 (2)	108 (3) *
TA Mass (mg)	41 (1)	37 (1) *
Soleus Mass (mg)	7.4 (0.3)	6.8 (0.2)
EDL Mass (mg)	9.7 (0.3)	9.1 (0.2)
Testes Mass (mg)	198 (3)	202 (4)
Heart Mass (mg)	156 (6)	143 (4)
Tibia (mm)	16.7 (0.1)	16.5 (0.1)

Data is expressed as mean (SEM). Abbreviations: PBS: Phosphate Buffered Saline, LLC: Lewis Lung Carcinoma, wks.: weeks, BW: body weight, g: grams, mg: milligrams, eWAT: epididymal white adipose tissue, and mm: millimeter, cm³/5 day: centimeters cubed per 5 days, pg/mL: picograms per milliliter, N.D.: Not detected, IL-6: Interleukin-6. Body weight change () is the following calculation (body weight end of study – tumor mass)/body weight day 10 in percent. Tumor growth rate is calculated as the tumor volume slope from days 15 to 25. Unpaired t-test was used to compare PBS to LLC.

* Different than PBS.

[^] different than pre tumor inoculation. Statistical significance was set a p<0.05.

Table 2:

Effect of LLC on Daily Average Indirect Calorimetry, Physical Activity, and Fuel Oxidation

	PBS	LLC
N	11	16
Time since Tumor Inoculation (wks.)	2.2	2.2
Tumor Volume Pre-CLAMs (cm³)	-	0.56 (0.01)
Tumor Volume Post CLAMs (cm³)	-	1.61 (0.18)
<i>Body Weight</i>		
Body Weight Pre-CLAMs (g)	26.0 (0.6)	27.2 (0.5)
Body Weight Post-CLAMs (g)	25.3 (0.6)	26.4 (0.6)
BW Change during CLAMs (%)	-2.8 (0.7)	-2.6 (1.0)
<i>Body Composition Pre</i>		
Lean Mass (g)	23.0 (0.6)	24.1 (0.5)
Fat Mass (g)	2.4 (0.2)	2.4 (0.1)
<i>Metabolic Parameters: Daily Average</i>		
Relative VO₂ (ml/kg lean mass/hr)	3977 (225)	4063 (166)
Absolute VO₂ (ml/hr)	91.5 (5.3)	97.6 (3.7)
Relative VCO₂ (ml/kg lean mass/hr)	3443 (191)	3456 (150)
Absolute VCO₂ (ml/hr)	79.0 (4.7)	83.0 (3.4)
Respiratory Exchange Ratio	0.860 (0.005)	0.847 (0.008)
Lipid Oxidation (g/min)	0.338 (0.028)	0.397 (0.024)
Carbohydrate Oxidation (g/min)	1.13 (0.08)	1.102 (0.075)
Energy Expenditure (kcal/kg lean mass/hr)	19.4 (1.1)	19.7 (0.8)
Heat Production (watts)	0.44 (0.03)	0.48 (0.02)
Food Intake (grams)	3.89 (0.23)	3.91 (0.47)
Cage Activity (counts)	11392 (866)	8713 (100) *

Data is expressed as mean (SEM). Metabolic Parameters are presented as the daily average. Abbreviations: PBS: Phosphate Buffered Saline, LLC: Lewis Lung Carcinoma, wks.: weeks, BW: body weight, g: grams, cm³: centimeters cubed, ml/kg lean mass/hr: milligrams per kilogram of lean mass per hour, g/min: grams per minute, VO₂: Oxygen consumption, VCO₂: Carbon Dioxide CLAMs: Comprehensive Laboratory Animal Monitoring System. Food intake was the average of food consumed over 5 days. Unpaired t-test was used to compare PBS to LLC.

* Different than PBS. Statistical significance was set a p<0.05.

Table 3:

Relationship of Tumor Growth and Indices of Cachexia on Physical Activity, Indirect Calorimetry and Fuel Utilization in LLC Mice.

Indices of Cachexia		Activity	RER	EE	VCO2	VO2	Lipid Oxidation	CHO Oxidation
Tumor Mass								
<i>Average Daily</i>	Figure 5B	-0.348	0.157	0.151	0.223	0.335	-0.074	
<i>Dark Cycle</i>		-0.371	-0.259	0.200	0.208	0.279	0.286	-0.191
<i>Light Cycle</i>		-0.700 *	-0.332	0.084	0.089	0.146	0.187	-0.288
BW d10								
<i>Average Daily</i>		0.410	0.471	-0.191	-0.202	-0.301	<i>-0.464</i>	0.125
<i>Dark Cycle</i>		0.320	0.383	-0.199	-0.228	-0.331	-0.421	0.221
<i>Light Cycle</i>		0.520 *	<i>0.503</i>	-0.168	-0.168	-0.251	-0.329	0.330
Hindlimb Muscle Mass								
<i>Average Daily</i>	Figure 5D	0.823 *	-0.041	-0.082	-0.254	-0.791 *	0.451	
<i>Dark Cycle</i>		0.590 *	0.827 *	0.012	-0.025	-0.215	-0.856 *	<i>0.461</i>
<i>Light Cycle</i>		0.615 *	0.684 *	-0.116	-0.173	-0.289	<i>-0.484</i>	0.409
eWAT								
<i>Average Daily</i>		0.620 *	0.521 *	-0.011	-0.064	-0.177	-0.515 *	0.338
<i>Dark Cycle</i>		0.598 *	0.604 *	0.066	0.023	-0.111	-0.596 *	0.282
<i>Light Cycle</i>		0.592 *	0.272	-0.125	-0.198	-0.244	-0.249	0.091
Plasma IL-6								
<i>Average Daily</i>	Figure 5E	-0.560 *	0.080	-0.205	-0.028	0.451	-0.202	
<i>Dark Cycle</i>		<i>-0.457</i>	-0.633 *	0.116	-0.262	-0.071	0.617 *	-0.160
<i>Light Cycle</i>		-0.548 *	-0.273	0.003	-0.101	0.024	0.203	-0.167

Data is expressed as r correlation value. Abbreviations: eWAT: epididymal white adipose tissue, BW d10: Body weight change is the (body weight end of study – tumor mass)/body weight day 10 in percent, RER: respiratory exchange ratio, EE: Energy expenditure, VO2: Oxygen consumption, VCO2: Carbon Dioxide, CHO: carbohydrate. Pearson Correlation Coefficient was used for correlations.

* And bolded indicate variables are significantly correlated. Correlations trending to be significant $p < 0.100$ are italicized. Statistical significance was set a $p < 0.05$. N=15.